# Graphene-on-silver substrates for sensitive surface plasmon resonance imaging biosensors

Seung Ho Choi,[1] Young L. Kim,[1] and Kyung Min Byun[2,*]

[1]*Weldon School of Biomedical Engineering, Purdue University, West Lafayette, Indiana 47907, USA*
[2]*Department of Biomedical Engineering, Kyung Hee University, Yongin, 446-701, Korea*
*\*kmbyun@khu.ac.kr*

**Abstract:** Taking advantage of the high impermeability property of graphene and the sharp surface plasmon resonance (SPR) curve of silver, we numerically demonstrate that SPR imaging biosensors with a graphene-on-silver substrate can be used to achieve the dramatically high sensitivity as well as to prevent silver oxidation. Results of our numerical study show that a silver substrate with a few graphene layers can significantly increase the imaging sensitivity, compared to the conventional gold-film-based SPR imaging biosensor. In particular, single layered graphene deposited on the 60-nm thick silver film amplifies the SPR imaging signal more than three times. Therefore, the proposed SPR substrate could potentially open a new possibility of SPR imaging detection for sensitive and high-throughput assessment of multiple biomolecular interactions.

©2011 Optical Society of America

**OCIS codes:** (280.4788) Optical sensing and sensors; (240.6680) Surface plasmons; (310.0310) Thin films.

## References and links

1. J. Homola, S. S. Yee, and G. Gauglitz, "Surface plasmon resonance sensors: review," Sens. Actuators B Chem. **54**(1-2), 3–15 (1999).
2. J. Homola, "Present and future of surface plasmon resonance biosensors," Anal. Bioanal. Chem. **377**(3), 528–539 (2003).
3. N. Blow, "Proteins and proteomics: life on the surface," Nat. Methods **6**(5), 389–393 (2009).
4. H. J. Lee, D. Nedelkov, and R. M. Corn, "Surface plasmon resonance imaging measurements of antibody arrays for the multiplexed detection of low molecular weight protein biomarkers," Anal. Chem. **78**(18), 6504–6510 (2006).
5. K. M. Byun, M. L. Shuler, S. J. Kim, S. J. Yoon, and D. Kim, "Sensitivity enhancement of surface plasmon resonance imaging using periodic metallic nanowires," J. Lightwave Technol. **26**(11), 1472–1478 (2008).
6. B. H. Ong, X. Yuan, S. C. Tjin, J. Zhang, and H. M. Ng, "Optimised film thickness for maximum evanescent field enhancement of a bimetallic film surface plasmon resonance biosensor," Sens. Actuators B Chem. **114**(2), 1028–1034 (2006).
7. X.-M. Zhu, P.-H. Lin, P. Ao, and L. B. Sorensen, "Surface treatments for surface plasmon resonance biosensors," Sens. Actuators B Chem. **84**(2-3), 106–112 (2002).
8. S. H. Choi and K. M. Byun, "Investigation on an application of silver substrates for sensitive surface plasmon resonance imaging detection," J. Opt. Soc. Am. A **27**(10), 2229–2236 (2010).
9. P. Avouris, Z. Chen, and V. Perebeinos, "Carbon-based electronics," Nat. Nanotechnol. **2**(10), 605–615 (2007).
10. C. W. J. Beenakker, "*Colloquium*: Andreev reflection and Klein tunneling in graphene," Rev. Mod. Phys. **80**(4), 1337–1354 (2008).
11. A. K. Geim and K. S. Novoselov, "The rise of graphene," Nat. Mater. **6**(3), 183–191 (2007).
12. K. S. Novoselov, A. K. Geim, S. V. Morozov, D. Jiang, Y. Zhang, S. V. Dubonos, I. V. Grigorieva, and A. A. Firsov, "Electric field effect in atomically thin carbon films," Science **306**(5696), 666–669 (2004).
13. J. S. Bunch, S. S. Verbridge, J. S. Alden, A. M. van der Zande, J. M. Parpia, H. G. Craighead, and P. L. McEuen, "Impermeable atomic membranes from graphene sheets," Nano Lett. **8**(8), 2458–2462 (2008).
14. D. E. Jiang, V. R. Cooper, and S. Dai, "Porous graphene as the ultimate membrane for gas separation," Nano Lett. **9**(12), 4019–4024 (2009).
15. L. Wu, H. S. Chu, W. S. Koh, and E. P. Li, "Highly sensitive graphene biosensors based on surface plasmon resonance," Opt. Express **18**(14), 14395–14400 (2010).
16. D. E. Gray, S. C. Case-Green, T. S. Fell, P. J. Dobson, and E. M. Southern, "Ellipsometric and interferometric characterization of DNA probes immobilized on a combinatorial array," Langmuir **13**(10), 2833–2842 (1997).
17. S. Elhadj, G. Singh, and R. F. Saraf, "Optical properties of an immobilized DNA monolayer from 255 to 700 nm," Langmuir **20**(13), 5539–5543 (2004).
18. E. D. Palik, *Handbook of Optical Constants of Solids* (Academic, 1985).

19. M. Bruna and S. Borini, "Optical constants of graphene layers in the visible range," Appl. Phys. Lett. **94**(3), 031901 (2009).
20. A. Yariv and P. Yeh, *Optical Waves in Crystals: Propagation and Control of Laser Radiation* (Wiley, 1984).
21. I. Pockrand, "Surface plasma oscillations at silver surfaces with thin transparent and absorbing coatings," Surf. Sci. **72**(3), 577–588 (1978).
22. X. Li, X. Wang, L. Zhang, S. Lee, and H. Dai, "Chemically derived, ultrasmooth graphene nanoribbon semiconductors," Science **319**(5867), 1229–1232 (2008).
23. X. Liang, Z. Fu, and S. Y. Chou, "Graphene transistors fabricated via transfer-printing in device active-areas on large wafer," Nano Lett. **7**(12), 3840–3844 (2007).
24. J. Wintterlin, and M.-L. Bocquet, "Graphene on metal surfaces," Surf. Sci. **603**(10-12), 1841–1852 (2009).
25. L. Song, L. Ci, W. Gao, and P. M. Ajayan, "Transfer printing of graphene using gold film," ACS Nano **3**(6), 1353–1356 (2009).
26. J. C. Shelton, H. R. Patil, and J. M. Blakely, "Equilibrium segregation of carbon to a nickel (111) surface: A surface phase transition," Surf. Sci. **43**(2), 493–520 (1974).
27. M. Eizenberg and J. M. Blakely, "Carbon monolayer phase condensation on Ni(111)," Surf. Sci. **82**(1), 228–236 (1979).
28. A. I. Stognij, N. N. Novitskii, S. D. Tushina, and S. V. Kalinnikov, "Preparation of ultrathin gold films by oxygen-ion sputtering and their optical properties," Tech. Phys. **48**(6), 745–748 (2003).
29. Z. M. Qi, S. Xia, and H. Zou, "Slow spontaneous transformation of the morphology of ultrathin gold films characterized by localized surface plasmon resonance spectroscopy," Nanotechnology **20**(25), 255702 (2009).
30. B. Song, D. Li, W. Qi, M. Elstner, C. Fan, and H. Fang, "Graphene on Au(111): a highly conductive material with excellent adsorption properties for high-resolution bio/nanodetection and identification," ChemPhysChem **11**(3), 585–589 (2010).
31. C. Leung, H. Kinns, B. W. Hoogenboom, S. Howorka, and P. Mesquida, "Imaging surface charges of individual biomolecules," Nano Lett. **9**(7), 2769–2773 (2009).

## 1. Introduction

Surface plasmons are collective oscillations of free electrons that propagate along a thin metal film when it is in contact with a dielectric interface. At a specific incidence angle, the momentum matching between the incident photon and the surface plasmon is achieved and the surface plasmon resonantly couples with the incident light, which is called surface plasmon resonance (SPR) [1]. The incidence angle where there is complete attenuation of the reflected light is referred to as the SPR angle and its position is dependent on the refractive index of a sensing medium. Since SPR is a rapid, sensitive, and label-free technique that can provide real-time data on adsorption events, SPR-based optical biosensors have been extensively used to study biomolecular interactions occurring at a metal/dielectric interface [2].

Among several instrumental SPR biosensing platforms, the most widely used format is the angle interrogation scheme, in which the reflectivity of monochromatic light is monitored as a function of the incidence angle. This approach has been known to be robust and sensitive, in part because commercially available instrumentations allow angular resolutions as low as 0.001°. However, a serious disadvantage is that the scanning angle type cannot provide the capability of screening diverse sets of biomolecular interactions at a time [3]. To overcome this limitation, SPR imaging schemes without any moving components at a fixed incidence angle are often used to measure the spatial changes in reflectivity. Indeed, this unique property of SPR imaging offers an attractive tool for monitoring numerous interactions in a parallel manner [4,5].

Generally, a silver film with a sharp SPR curve may yield a higher imaging sensitivity than a gold film [6]. However, the sensitivity of the SPR imaging biosensor has a potential limitation, because silver is highly susceptible to oxidation. While the use of a thin gold film might be a better choice in terms of stability and reliability, silver would be a promising candidate for sensitive SPR imaging detection if silver surfaces can be made chemically inert [7]. Despite the great sensitivity of a silver film, when a homogeneous silver oxide layer is formed by processing the silver film in an oxygen-containing atmosphere, the imaging sensitivity is decreased with an increasing silver oxide thickness because the oxide coating makes SPR curves broader [8].

In this respect, we have been searching for possible methods to prevent the oxidation of the silver film in SPR imaging biosensor. We paid attention to graphene, given that the unique properties of graphene sheets and their potential applications have been the objective of

intensive investigation [9–11] since the successful isolation of single atomic planes of graphite in 2004 [12]. In particular, we notice that the graphene sheet is impermeable to gases as small as He [13]. This is attributed to the fact that the electron density of hexagonal rings is substantial enough to prevent atoms and molecules from passing through the ring structure [14]. Therefore, we hypothesize that by coating a silver film with graphene, no passing-through events of oxygen gases can occur and thus, the graphene will protect the silver substrate from oxidation.

The recent numerical study by Wu et al. reported that a graphene-on-gold SPR biosensor can be more sensitive than the conventional gold film-based biosensors, due to the increased adsorption of target biomolecules on graphene [15]. However, the following key issues have not been addressed for the development of the graphene-on-silver SPR biosensors in an imaging mode: 1) What is the sensitivity limit of the graphene-on-silver substrate for biomolecular detection? It should be noted that a graphene layer will be truly useful on a silver film, because graphene can prevent the oxidization of the silver substrate while maintaining the high sensitivity induced from the silver substrate. 2) What is the optimal structure of the graphene-based SPR substrate to maintain the high sensitivity? A significant number of graphene layers will make an SPR curve broader and consequently aggravate the imaging sensitivity. 3) Does the SPR imaging signal show a linear shift in a wide range of the refractive index variations? In addition to the high sensitivity, a greatly linear sensing performance is required for quantitative monitoring of biomolecular interactions.

In this study, we, for the first time to our knowledge, propose the concept of the graphene-on-silver substrate as an alternative, yet effective, SPR structure. Our numerical study reveals that this scheme has the great potential for improving the sensing performance of the silver-based SPR imaging biosensors, superior to the conventional gold-based SPR imaging biosensors. Thus, our study will serve as the first step to demonstrate the feasibility of the oxidation-free graphene-on-silver substrate for sensitive SPR imaging detection.
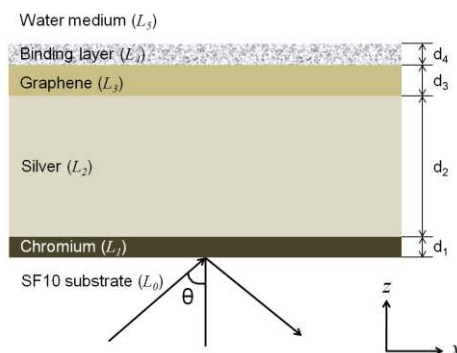
## 2. Numerical model



Fig. 1. Schematic of a SPR imaging configuration based on a graphene-on-silver substrate. A silver film ($d_2$) is deposited on a SF10 prism substrate via adhesion of a chromium layer ($d_1 = 2$ nm). Graphene layers ($d_3$) are coated on the silver film and binding analytes of DNA hybridization ($d_4 = 3$ nm) are modeled as a homogeneous layer with an initial refractive index of 1.462 in a water medium [16,17].

Figure 1 shows a schematic of the proposed graphene-on-silver SPR biosensor. A uniform silver film is coated on a SF10 glass prism via an attachment of 2-nm thick chromium layer. A biomolecular reaction of DNA hybridization is modeled as a 3-nm-thick dielectric layer that covers the whole graphene surface. At an initial stage, the refractive index of an immobilized single-stranded DNA (ss-DNA) is set to be 1.462 and this value gradually increases with the degree of the double-stranded DNA (ds-DNA) formation. The refractive index of the DNA layer was estimated from the results of ellipsometric characterizations for 27-mer ss-DNA and its complementary target DNA [16,17]. TM-polarized light at the wavelength $\lambda = 633$ nm illuminates the substrate at a predetermined incidence angle that produces a maximal intensity

change. The optical constants $\varepsilon = (n, k)$ of SF10 substrate and thin layers of chromium and silver are set to be (1.723, 0), (3.48, 4.36), and (0.059, 4.243), respectively, at $\lambda$ = 633 nm [18]. Recently, the dielectric function of graphene in the visible range was estimated to be $n$ = 3.0 and $k = C_1\lambda/3$ with $C_1$ = 5.446 $\mu m^{-1}$ [19], which can be useful for accurate prediction of the optical behavior of graphene structures. In our calculation, the graphene layer is presumed to be homogeneous and its thickness is equal to $d_3$ = N × 0.34 nm, where N is the number of graphene sheets.

To numerically obtain the optical characteristics of the graphene-based SPR biosensor, we used the transfer-matrix method (TMM) [20]. Assuming that biomolecular reactions produce a change in refractive index $n_4$ of the binding layer and do not induce a change in thickness, a variance of reflectance $R$ occurs as $n_4$ increases and thus, the sensitivity of the SPR imaging biosensor can be defined as $S = dR/dn_4$. When the TM-polarized light is incident to the SPR imaging system at an angle $\theta$ as shown in Fig. 1, the reflectance $R$ is represented by 2 × 2 $M$-matrix, which is a serial product of the interface matrix $I_{jk}$ ($j$ = 0, 1, 2, 3, and 4 with $k = j + 1$) and the layer matrix $L_j$. Then the imaging sensitivity $S$ is obtained by differentiating the reflectance $R$ directly with respect to $n_4$ as follows:

$$S = \frac{dR}{dn_4} = \frac{d}{dn_4}\left|\frac{M_{12}}{M_{22}}\right|^2 , \qquad (1)$$

where

$$M = \begin{bmatrix} M_{11} & M_{12} \\ M_{21} & M_{22} \end{bmatrix} = I_{01}L_1I_{12}L_2I_{23}L_3I_{34}L_4I_{45},$$

$$I_{jk} = \begin{bmatrix} 1 & r_{jk} \\ r_{jk} & 1 \end{bmatrix} \text{ and } L_j = \begin{bmatrix} e^{ik_{zj}d_j} & 0 \\ 0 & e^{-ik_{zj}d_j} \end{bmatrix}. \qquad (2)$$

Here, $r_{jk}$, $k_{zj}$, and $d_j$ represent the Fresnel reflection coefficient, the wave-vector in the z-direction, and the thickness of $j$-th layer, respectively. $r_{jk}$ and $k_{zj}$ are given by

$$r_{jk} = \frac{\left(\dfrac{k_{zj}}{\varepsilon_j} - \dfrac{k_{zk}}{\varepsilon_k}\right)}{\left(\dfrac{k_{zj}}{\varepsilon_j} + \dfrac{k_{zk}}{\varepsilon_k}\right)} \text{ and } k_{zj} = \sqrt{\varepsilon_j\left(\frac{\omega}{c}\right)^2 - k_x^2} \text{ with } k_x = \sqrt{\varepsilon_0}\frac{\omega}{c}\sin\theta, \qquad (3)$$

where $\omega$ is the angular frequency, $c$ is the speed of light in free-space, and $\varepsilon_j$ is the optical constant of the $j$-th layer.

## 3. Numerical results

### 3.1 Overall comparison of imaging sensitivity between silver and gold substrates

Using our TMM model, the reflectance and sensitivity curves of silver or gold substrates are calculated to compare their imaging characteristics, when the monochromatic light is incident into the 40-nm thick silver or gold films in a water solution.
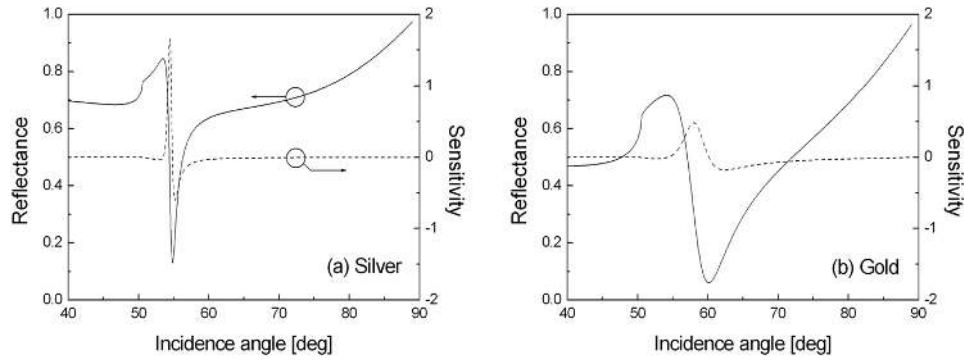
Fig. 2. SPR reflectance (solid lines) and its sensitivity (dashed lines) for (a) silver and (b) gold substrates. In this calculation, TM-polarized light at λ = 633 nm propagating into the SF10 prism substrate is incident on the thin silver or gold film (40 nm) in the water solution.

Figure 2 shows two incidence angles with positive and negative peak sensitivities for both metallic substrates, at which the change in the reflectance signal reaches a maximum. In particular, since the gradient in reflectivity is steeper for the incidence angle preceding the resonance angle, the magnitude of the positive peak is generally larger than that of the negative one. Hence, the predetermined incidence angle in SPR imaging is equivalent to the condition in which this positive peak is obtained. At the resonance position with a minimum reflectance, the sensitivity, however, becomes almost zero because its slope (i.e., the gradient of the reflectivity) is horizontally flat. In Fig. 2, another important aspect is that the silver substrate is obviously advantageous in terms of the imaging sensitivity compared to the gold substrate. The peak sensitivity of the gold surface is found to be 0.483, while the silver film has a maximum sensitivity of 1.653 at the incidence angle of 54.5°, implying a 3.4 times better sensitivity. In addition to the narrow SPR curve of the silver film, resonant plasmon excitations prompted by photons with a smaller incidence angle are partly attributable to the higher imaging sensitivity of the silver substrates.
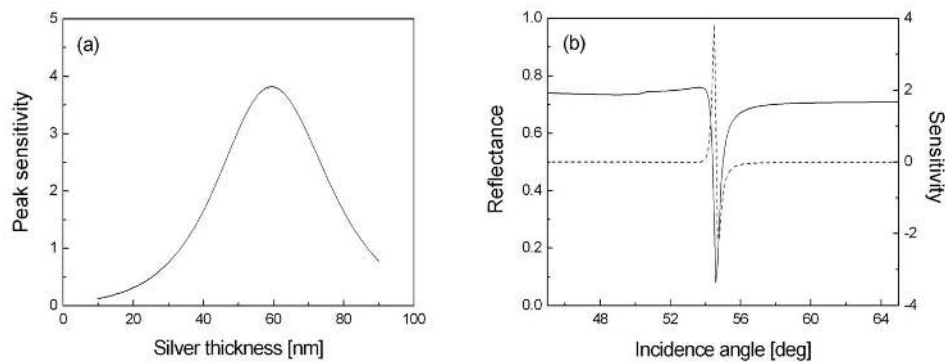


Fig. 3. (a) Plot of the peak SPR imaging sensitivity as a function of the silver thickness when graphene sheets are not applied. (b) SPR reflectance and sensitivity characteristics in the case of an optimal silver thickness of $d_2 = 60$ nm with the highest imaging sensitivity of $S = 3.82$.

*3.2 Effect of graphene layers on SPR imaging sensitivity*

Based on the result of the outstanding sensitivity performance of the silver film, we further calculated the peak values of the imaging sensitivity as a function of the silver thickness $d_2$ when $d_3 = 0$ nm and $n_4 = 1.462$ (i.e., ss-DNA probes are directly immobilized on a silver substrate).

In Fig. 3(a), the maximum sensitivity was obtained to be as high as 3.82 at an optimal thickness of $d_2 = 60$ nm. In the case of thin-gold-film-based SPR imaging detection, its peak

sensitivity equals 0.68 at the gold thickness of 56 nm, whose sensitivity is 5.6 times lower than that of the silver substrate. However, the previous study found that, when an oxidation occurs and silver oxide is produced on a silver film, this significant sensitivity of the silver substrate can be decreased with an increase in the silver oxide thickness [8]. In other words, since thicker oxide layers lead to a resonance excitation of surface plasmons in a higher momentum, the sharp SPR curve in Fig. 3(b) becomes broader and shallower, resulting in a notable degradation of the imaging sensitivity.
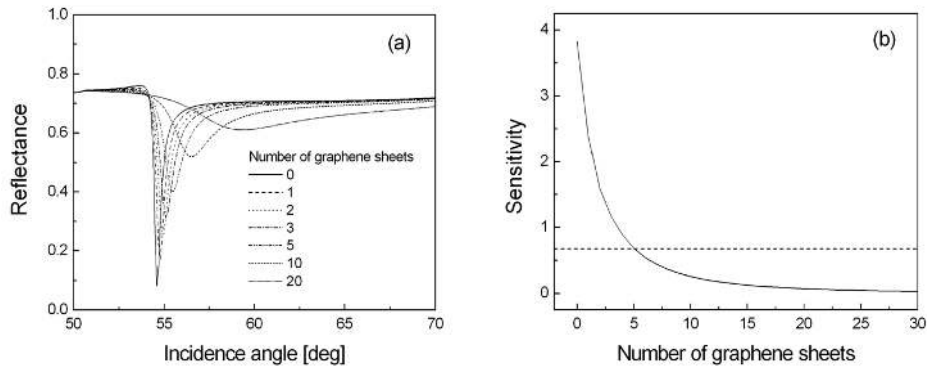


Fig. 4. (a) SPR reflectance and (b) peak imaging sensitivity as the number of graphene layers increases. The dashed line in (b) indicates the highest imaging sensitivity of 0.68 obtained from the conventional gold-film-based SPR substrate.

Hence, in order to protect the silver substrate from oxidation, we applied a graphene sheet, which has been known to be impermeable to oxygen, to an SPR imaging structure. Figure 4 shows the characteristics of the reflectance and imaging sensitivity as a function of the number of graphene sheets when the silver film has a thickness of $d_2 = 60$ nm. In Fig. 4(a), the resonance angle increases with the graphene thickness in the range from 54.6° at $d_3 = 0$ to > 59° for thick graphene layers of $d_3 > 6$ nm. Also, the reflectivity becomes broader and shallower with an increase in the graphene layer. These changes in the SPR angle, the curve width, and the magnitude of reflectivity resemble the dramatic variations in the SPR signal induced by thin carbon coatings evaporated onto silver films [21]. Similar absorptive plasmon damping associated with graphene sheets may be responsible for the obtained SPR changes, because the graphene sheet possesses a nonzero imaginary dielectric component. This absorption effect is confirmed by the calculation results in Fig. 4(b), demonstrating an exponential decay of the imaging sensitivity. Although degradation of the imaging sensitivity caused by a higher resonance angle and correspondingly broader and shallower SPR curves is unavoidable, it should be emphasized that a monolayer or bilayer of graphene sheet can provide exceptional sensitivities, which are 3.5 or 2.1 times larger than the highest sensitivity for the conventional gold substrates (the dashed line in Fig. 4).

*3.3 Structural optimization of graphene-based SPR imaging substrates*

To optimize the design of the graphene-based SPR imaging biosensor, we calculated the peak sensitivity at wide ranges of the silver film thickness and the number of graphene sheets, as shown in Fig. 5. The sensitivity is generally decreased with the increase in the number of graphene sheets and this trend is consistent with the results in Fig. 4. It is, therefore, important to realize an extremely thin graphene layer, so that the sensitivity obtained from bare silver substrates would not be degenerated significantly by the introduction of graphene sheets. Fortunately, many reliable fabrication techniques have been developed for isolating individual single or few-layer graphene from graphite successfully [12,22,23], although there are still technical difficulties to be resolved to easily manipulate and transfer graphene on a large scale. Assuming that silver substrates with mono- or bi-layered graphene sheets are practically feasible, the sensitivity of the graphene-on-silver substrates exhibits a better performance than

that of the gold substrate at the wide range of silver film thickness, shown in the white dashed line in Fig. 5. Overall, the proposed substrate could potentially be used as an effective alternative to achieve a high imaging sensitivity as well as to prevent silver oxidation.
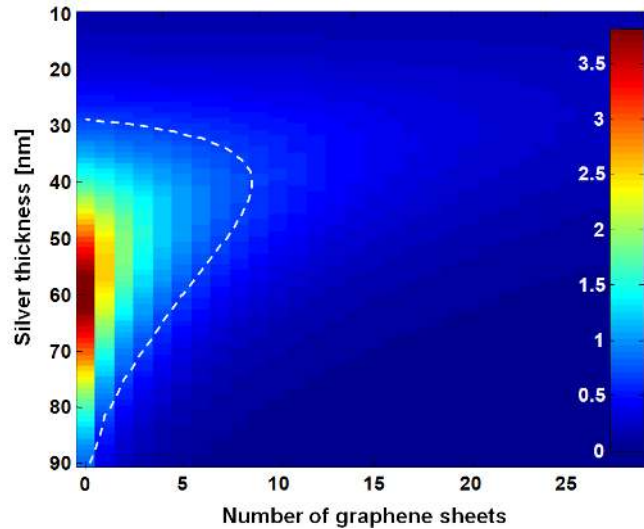


Fig. 5. Peak sensitivity of SPR imaging as the silver film thickness varies from 10 to 90 nm and the number of graphene layers increases up to 30. The white dashed line indicates the condition that the peak imaging sensitivity of the graphene-on-silver substrate is equivalent to the maximum imaging sensitivity of 0.68, obtained from the gold-film-based SPR imaging substrate.

Moreover, we found that for 40 nm $\leq$ $d_3$ $\leq$ 50 nm, the imaging sensitivity does not decrease rapidly with an increase in the graphene thickness. Thus, the graphene-on-silver substrate shows a better sensitivity than for the conventional gold film until the number of graphene sheets reaches more than 5. Those results support an interesting postulation that we may select the silver film thickness depending on the minimum number of graphene sheets coated on a silver film. In other words, if a single- or double-layered graphene sheet is available, it is obviously required to evaporate the silver film with the thickness of $d_2$ ~60 nm. On the other hand, if an actual fabrication process of ultrathin graphene layers cannot guarantee the number of graphene sheets to be less than 5, it is preferable to choose the silver film thickness at around 40 nm, while the maximally obtainable imaging sensitivity can be somewhat degenerated.

### 3.4. Numerical analyses on SPR imaging detection of DNA hybridization

We further compared the imaging sensitivities between graphene-on-silver and conventional gold substrates by calculating a change in the reflectance when the refractive index of the binding layer increases in accordance with the concentration of adsorbed analytes. In determining design parameters of the two types of SPR imaging substrates, the graphene-on-silver substrate is modeled as a monolayer graphene coated on a silver film with the thickness of 60 nm (i.e., the initial imaging sensitivity is highest). For the gold-film-based SPR imaging biosensor, the gold thickness is chosen to be 56 nm with the highest sensitivity when $n_4$ = 1.462 as described in Fig. 4(b). As mentioned in the section of **2. Numerical model**, the binding event of DNA hybridization was defined as a 3-nm-thick dielectric monolayer and its refractive index varied from 1.462 to 1.480 in the course of the hybridization reaction. The initial value of 1.462 corresponded to a ss-DNA layer with a density of 0.028 g/cm$^3$, obtained from the ellipsometry measurements [16,17]. After the hybridization events, the ds-DNA layer with a density of 0.061 g/cm$^3$ corresponded to the refractive index of 1.530 [17]. Assuming that the refractive index change is linear with the increase in the concentration of

the bound DNA molecules, we can estimate the absolute concentration of individual DNA layers at the corresponding refractive index, as shown in the *x*-axis of Fig. 6.

Figure 6 shows that, for the conventional gold substrate, the maximum reflectance change is 0.012, while the net contrast of the graphene-on-silver substrate is obtained to be 0.043. Using the linear regression analyses, the correlation coefficient R is equal to R = 0.9999 for all the substrates. In other words, the reflectance shift is completely linear over the wide range of the DNA hybridization reaction. More importantly, the graphene-on-silver substrate presents approximately three times greater imaging sensitivity than that of the traditional gold substrate.
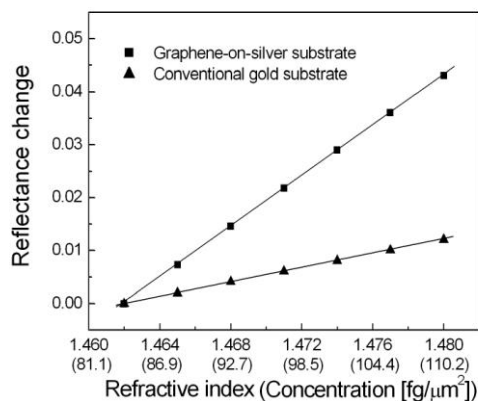


Fig. 6. Linear regression analyses between the reflectance and the refractive index of binding analytes for SPR imaging configurations with the graphene-on-silver substrate (square) and the gold substrate (triangle). As the refractive index of the binding layer increases from 1.462 to 1.480 in an interval of 0.003, the reflectance amplitude linearly increases. The absolute concentration, which is equivalent to the refractive index of the bound DNA molecules, is presented together with the refractive index. The solid lines denote the linear fits for the two types of the SPR imaging substrates.

## 4. Discussion

Graphene layers on metal surfaces can be implemented by two approaches [24]: 1) segregation of bulk-dissolved carbon to the surface and 2) surface decomposition of carbon-containing molecules. Based on these methods, single crystal metal substrates with adsorbed graphene were obtained for various metallic materials, such as cobalt, nickel, iridium, and platinum. More recently, graphene-on-gold has been fabricated by exfoliating graphene layers from highly oriented pyrolytic graphite (HOPG) [25]. After patterning the graphene on the HOPG surfaces by photolithography and $O_2$ plasma etching, a gold film is deposited and then a thermal releasing tape can be used to peel-off the gold film together with the graphene patterns. By applying the transfer-printing technique subsequently, graphene patterns can be tightly attached to other substrates over large areas. While a realization of graphene-on-silver has not been reported yet, there is strong evidence that the transfer-printing technique and mechanical exfoliation process can make it possible to obtain silver substrates with a few graphene layers or even a monolayer [25–27].

Although our numerical results show a graphene interface as an excellent candidate for highly sensitive silver-film-based SPR imaging biosensors, another possible approach for preventing silver oxidation is to implement gold-on-silver bimetallic substrates where protective gold coating is applied over the silver film. In the previous SPR studies, the bimetallic substrates, however, presented noticeable changes in the SPR curves for the gold thickness larger than 3 nm, such as a broad curve width and an increased minimum reflectance at resonance, and consequently lead to greatly reduced sensitivities [8]. Although ultrathin gold films can be obtained by sputtering a gold target by means of oxygen ion beam,

an existing problem is that the deposition rate less than a level of 1 nm/sec should be controlled precisely by varying the parameters of an ion source in a rough vacuum [28]. In particular, the possibility of slow and spontaneous transformation of the morphology for ultrathin gold films makes the bimetallic substrates improper for a sensitive SPR imaging detection. Qi et al. demonstrated that a thin gold film with a thickness smaller than 10 nm tends to change from the initially continuous layer to nanoporous or nanoparticle structures at room temperature without surface treatments. Moreover, these nanostructures can induce a localized surface plasmon (LSP) band [29]. Since the presence of LSP modes and their interaction with propagating surface plasmons may strongly influence the broad reflectivity spectrum and decrease the sensing contrast, the SPR imaging sensitivity would be deteriorated even more drastically by the morphology transformation of thin gold coatings.

Further, the graphene-on-silver substrate could potentially facilitate the applications of its electric conduction property to the identification of single biomolecules. For example, when the metallic substrate with a graphene coating was combined with the tip of atomic force microscopy (AFM) or scanning tunneling microscopy (STM), the signal-to-noise ratio of the measured electrical signals was found to be high enough to distinguish individual nucleobases of ss-DNA [30]. This was even better than the signal-to-noise ratio of the conventional metallic surface without the graphene film. Hence, with the help of conductive AFM or STM tips, the graphene-based SPR imaging substrate can serve as a multi-functional bio-platform, enabling high-accuracy sequencing of DNA strands as well as sensitive biosensing. These are the main advantages of the excellent electric conduction compared to the results obtained from nonconductive substrates, which could lead to ambiguous topological images [31].

## 5. Conclusion

In this numerical study, we explored a novel SPR imaging biosensor based on a graphene-on-silver substrate in terms of the imaging sensitivity characteristics. When no graphene sheet is employed, the peak imaging sensitivity was obtained to be as high as 3.82 with the silver thickness of 60 nm, presenting 5.6 times larger sensitivity than for the gold film. However, we found that the addition of a few graphene sheets decreases the sensitivity of the silver film due to an absorptive damping process caused by graphene with a nonzero imaginary part. Nonetheless, the high impermeability of graphene could potentially to be used as a protective layer that prevents undesired oxidation of silver. More importantly, the graphene-on-silver substrates with extremely thin graphene sheets exhibited an extremely high sensitivity. The SPR imaging sensitivity was increased up to 3 times higher in detecting DNA hybridization interactions, compared to the conventional gold substrate. Considering rapid advances in fabrication techniques, we envision that true realization of a single graphene sheet attached to silver surfaces. Its applications to a sensitive SPR imaging for a number of biomolecular reactions will be readily achieved.